Hindawi
Applied Bionics and Biomechanics
Volume 2021, Article ID 5512762, 11 pages
https://doi.org/10.1155/2021/5512762

Research Article

Biomechanical Performance of Menisci under Cyclic Loads

J.-G. Tseng[1], **B.-W. Huang**[2], **Y.-T. Chen**[2], **S.-J. Kuo**[3] and **G.-W. Tseng**[4]

[1]*Department of Leisure and Sports Management, Cheng Shiu University, Kaohsiung, Taiwan*
[2]*Department of Mechanical Engineering, Cheng Shiu University, Kaohsiung, Taiwan*
[3]*School of Medicine, China Medical University; Department of Orthopedic Surgery, China Medical University Hospital, Taichung, Taiwan*
[4]*School of Medicine, Medical College, China Medical University, Taichung, Taiwan*

Correspondence should be addressed to B.-W. Huang; huangbw@gcloud.csu.edu.tw

Received 12 January 2021; Revised 13 April 2021; Accepted 21 April 2021; Published 11 May 2021

Academic Editor: Nicola Francesco Lopomo

The meniscus, composed of fibrocartilage, is a very important part of the human knee joint that behaves like a buffer. Located in the middle of the femoral condyles and the tibial plateau, it is a necessary structure to maintain normal biomechanical properties of the knee. Whether walking or exercising, the meniscus plays a vital role to protect the articular surface of both the femoral condyles and the tibial plateau by absorbing the conveying shock from body weight. However, modern people often suffer from irreversible degeneration of joint tissue due to exercise-induced harm or aging. Therefore, understanding its dynamic characteristics will help to learn more about the actual state of motion and to avoid unnecessary injury. This study uses reverse engineering equipment, a 3D optical scanner, and a plastic teaching human body model to build the geometry of knee joint meniscus. Then, the finite element method (FEM) is employed to obtain the dynamic characteristics of the meniscus. The results show the natural frequencies, mode shapes, and fatigue life analysis of meniscus, with real human material parameters. The achieved results can be applied to do subsequent knee dynamic simulation analysis, to reduce the knee joint and lower external impacts, and to manufacture artificial meniscus through tissue engineering.

1. Introduction

The meniscus is an important tissue in the human knee joint because of its load distribution, shock absorption, joint lubrication, and joint stability functions. Meniscal damage, which may appear as tear, maceration, degeneration, or destruction, is frequently found from a common sports injury or the osteoarthritis (OA) knee. Approximately, 23% of all adults or more than 54 million people in the U.S. suffer from some form of wear and tear arthritis. The annual direct medical costs are at least $140 billion [1]. With the developments and changes in time, the joint injury should no longer be considered as a problem that only occurs in the elderly, as many of whom are young people the age of 20 to 30 years old. The usual treatments to repair the meniscus are using sutures or staples to restore the integrity of the tissue, partial meniscectomy, or biodegradable tissue adhesives [2]. The new strategy of meniscus reconstruction employs tissue engineering that combines cells, materials methods, engineering, and biochemical factors to restore, maintain, improve, or replace meniscus tissues with similar mechanical properties to the original one [3–5]. Given the increasing need of joint replacement, a rising interest in academia has driven researchers to take a deep insight into the development of the leg joints includes bones and cartilages.

For a long time, biomechanical scientists have been committed to establishing an accurate geometric module either with or without magnetic resonance imaging (MRI). FEM is employed for the knee or meniscus model later on for the dynamical analysis [6–9]. Meakin et al. [10] developed a finite element model of the knee meniscus to obtain the stress distribution of various geometrical and material properties on the behavior of the meniscus under compressive load. Freutel et al. [11] reviewed many papers about finite element modeling of soft tissues: material models, tissue interaction, and challenges. Musculoskeletal soft tissues, such as articular

cartilage, ligaments, knee meniscus, and intervertebral disk, were discussed in the reviewed papers. In that, quite a few researchers adopted the isotropic, linear elasticity material model to limit computational cost and numerical difficulties. Bendjaballah et al. [12] developed a three-dimensional finite element model of the human knee joint. This model consists of hard-bone structures, their articular cartilage layers, menisci, and principal ligaments. They obtained the principal-compressive stress distribution in the centroid of tibial cartilage elements for the meniscus joint with free axial rotation at 1000 N external load. In this study, we focused on finding the fundamental normal modes, i.e., natural (resonant) frequencies and mode shapes of the human meniscus, to understand the dynamic characteristics of the knee joint. Natural frequencies are the existing in or initiated by nature, not produced or affected artificially, in the mechanical and biological structure when in motion. The motion pattern of a system oscillating at its natural frequency is called the normal mode, i.e., all parts of the system move sinusoidally with that same frequency [13]. If the external excitation frequency near the natural frequency, the amplitude of the vibrating structure will increase with time until fracture occurred finally. That is why the natural frequency is crucial to be avoided from the normally encountered excitation frequency when designing and building biostructure via the tissue engineering process.

To enable the geometric module more comparable to the complex motions of the natural knee, Pereira et al. [14] carried out dynamic mechanical analysis (DMA) with anterior, middle, and posterior segments of fresh menisci to regenerate meniscus lesions using tissue engineering strategies. Lots of related tissue engineering papers can also be found in the review articles [15, 16]. Tissue engineering using natural or synthetic matrices as a scaffold to guide tissue repair or regeneration in three dimensions shows promising prospects for meniscus regeneration [17]. With a scaffold being the basis of new tissue structure [18, 19], multiple ingredients are used in building a scaffold of the meniscus, including polyglycolic acid (PGA) and poly-L-lactic acid (PLA), and natural biological products, such as silk, collagen type I, and proteoglycans [20–22]. Our research results acquired the mechanical features of the human meniscus from the finite element modeling that can be compared and evaluated with those obtained from the regenerating meniscus by tissue engineering.

As the tribological phenomenon played a significant role in mechanical and clinical scenarios, Villa et al. [23] addressed the long-term structural integrity of metal tibial components in terms of fatigue life utilizing experimental tests and FEM simulations. To apprehend and avoid lower normal modes are the basic requirement to design the artificial joint, this article also shows the fatigue behavior under the 1000 N cyclic load on the menisci via daily movement.

This research studies how the numerical modal analysis, a nondestructive tool, characterizes and quantifies the fatigue behavior of human menisci [24] (Figure 1) by employing reverse engineering and FEM analysis. The response of modal parameters (damping ratio, natural (resonance) frequency, and mode shapes) is obtained to assess the variations in the meniscus. From the author's previous study of impact

Figure 1: Meniscus schematic diagram [24].

Figure 2: Breuckmann SmartSCAN 3D scanner.

analysis to the knee model, the highest compression stress occurred in the area of soft tissue—meniscus [25, 26]. It will be the main factor affecting the fatigue life of the meniscus. That helps to correlate the modal parameters and fatigue behavior [27]. Also, it applied cyclic stress loads and fatigue analysis to build simpler models with a fewer degree of freedom.

2. Materials and Methods

2.1. Geometry. Many researchers use a 3D scanning technique to obtain the precise geometric model for the FEM analysis. Fernandez et al. [28] developed a FEM model from the 3D optical scanning results to investigate the failure process and the variation of the mechanical properties in corroded steel reinforcement.

This research used a straightforward way by adopting a typical accurate teaching synthesis human knee joint model manufactured by 3B Incorporation, made in plastic material (polypropylene). The meniscus, a physical component of the knee-joint model, is reconstructed by the reverse engineering method. Based on the triangular optical detection principle, a 3D white light scanner, Breuckmann SmartSCAN 3D (Figure 2), is employed to access the outer profile of the components of the teaching synthesis plastic meniscus. The accuracy, volumetric accuracy, and measurement resolution of the SmartSCAN 3D are 0.05 mm, 0.05 mm, and 0.1 mm,

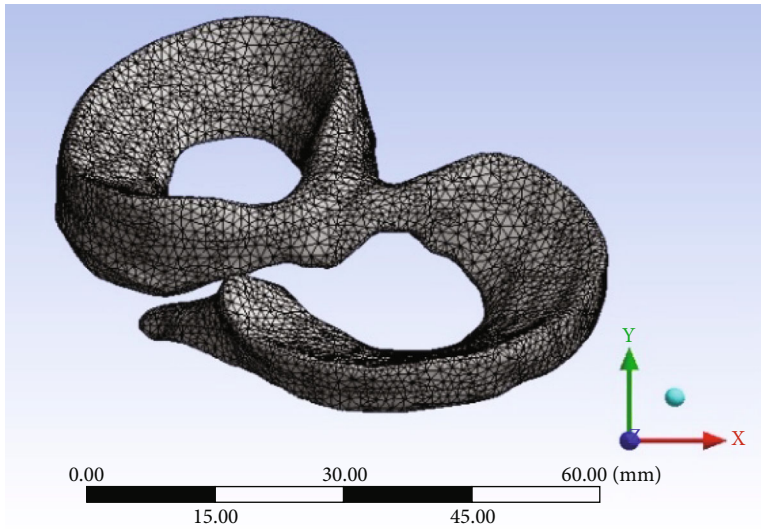

Figure 3: FEM mesh of the meniscus.

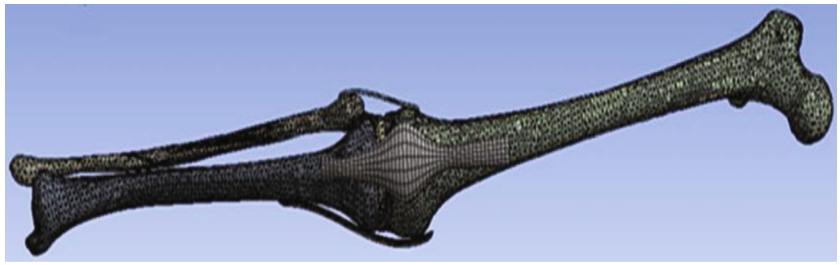

Figure 4: FEM mesh of the complete knee model (CKM) [25].

respectively. Despite its high resolution, there still exist holes, bumps, and crinkles on the surface of the model after each scanning. The rough surface geometry of the scanned meniscus model is filled and smoothed, respectively, by the Geomagic Studio software. This smoothed geometry of the meniscus model is ready to be imported into the finite element software package.

2.2. Dynamic Analysis. This study utilized the FEM software ANSYS of various modules to analyze dynamic characteristics of the 3D meniscal model includes natural vibration frequencies, mode shapes, and fatigue life limitation. There is an infinite number of natural frequencies and accompany mode shapes that existed in a continuous multidegree of freedom structure. Only the first couple of fundamental natural frequencies/modes is usually encountered by the external driving force and are important for the analysis. Dynamic analysis for simple structures can be carried out manually, but for complex structures like menisci, finite element analysis is usually used to calculate their mode shapes and frequencies.

The finite element analysis included importing the built model, meshing, setting up meniscus parameters and boundary conditions, and proceeding element convergence test. The scanned model of the meniscus is imported into the ANSYS finite element software and using the Solid186 element for soft tissues. It can adjust the coarseness of the mesh through the size and shape of the element and will affect the correctness of the analysis. The authors used ANSYS intelligent mesh Element-strengthen technology to ensure accuracy. Figure 3 shows the meniscus FEM mesh used for modal analysis under free boundary conditions.

Table 1: Real human material parameters [29–34].

Components	Young's modulus MPa	Poisson's ratio	Density kg/m^3
Bone	17,000	0.3	2,132.6
Meniscus	59.0	0.49	1,024.0
Anterior cruciate ligament (ACL)	366.0	0.45	1,100.0
Posterior cruciate ligament (PCL)	131.5	0.45	1,100.0
Patellar tendon	116.0	0.45	1,100.0
Lateral ligament	366.0	0.45	1,100.0

Table 2: First four flexible vibration natural frequencies of meniscus model.

Mode	Flexible natural frequencies (Hz)
1	72.4
2	91.8
3	127.1
4	184.1

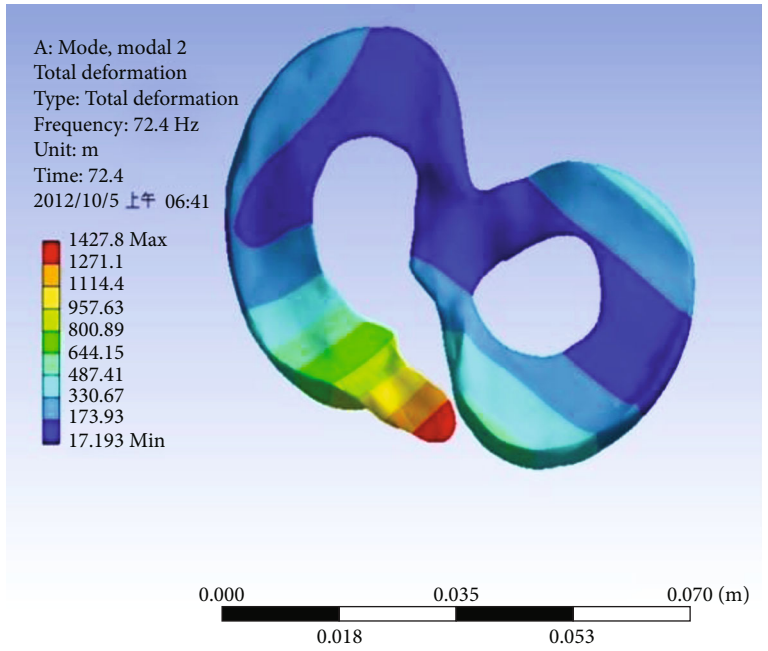

(a)

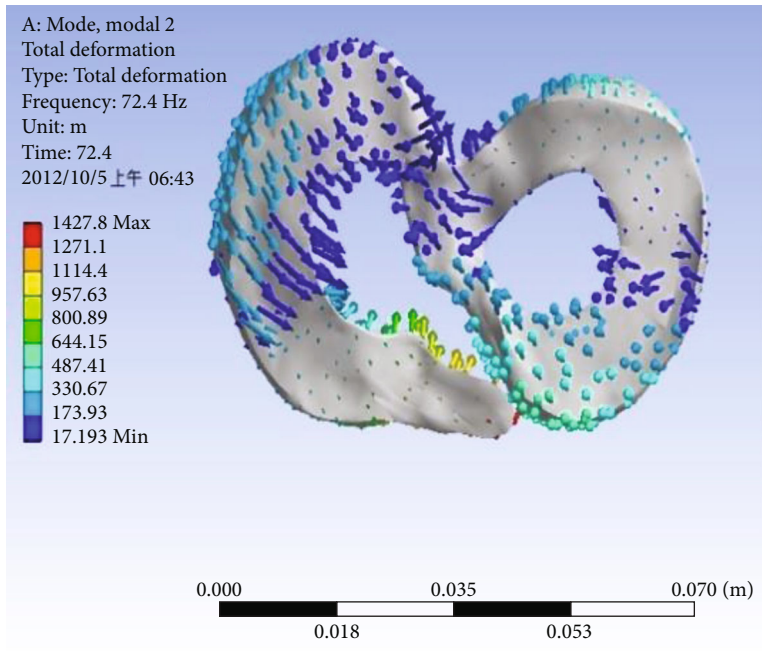

(b)

Figure 5: First mode shape of meniscus model at 72.4 Hz (bending vibration via thickness direction). (a) First mode shape. (b) Vector plot of first mode shape.

Fatigue is the weakening of a material caused by repetitive loadings. When applies cyclic loading to material, continuous and localized structural damage will occur. The nominal maximum stress which causes such damage may be much less than the ultimate tensile stress limit. If the loads are higher than a certain threshold, microscopic cracks will begin to form at places of stress concentration. Eventually, the crack will propagate suddenly when it reaches a critical size, and the structure will fracture [27]. To find fatigue life limitation satisfies the real motion situation, the new scanned meniscus model is combined with the authors' previous work [25], consisted of femur, tibia, knee cap, anterior ligament, posterior ligament, and lateral ligament, to form a complete knee model (CKM), as shown in Figure 4. The complete knee model (CKM) has three purposes: (1) to determine the minimum number of meshed element for the model by evaluating the convergence of the natural frequency of the CKM, (2) to check the correctness of the analysis by comparing

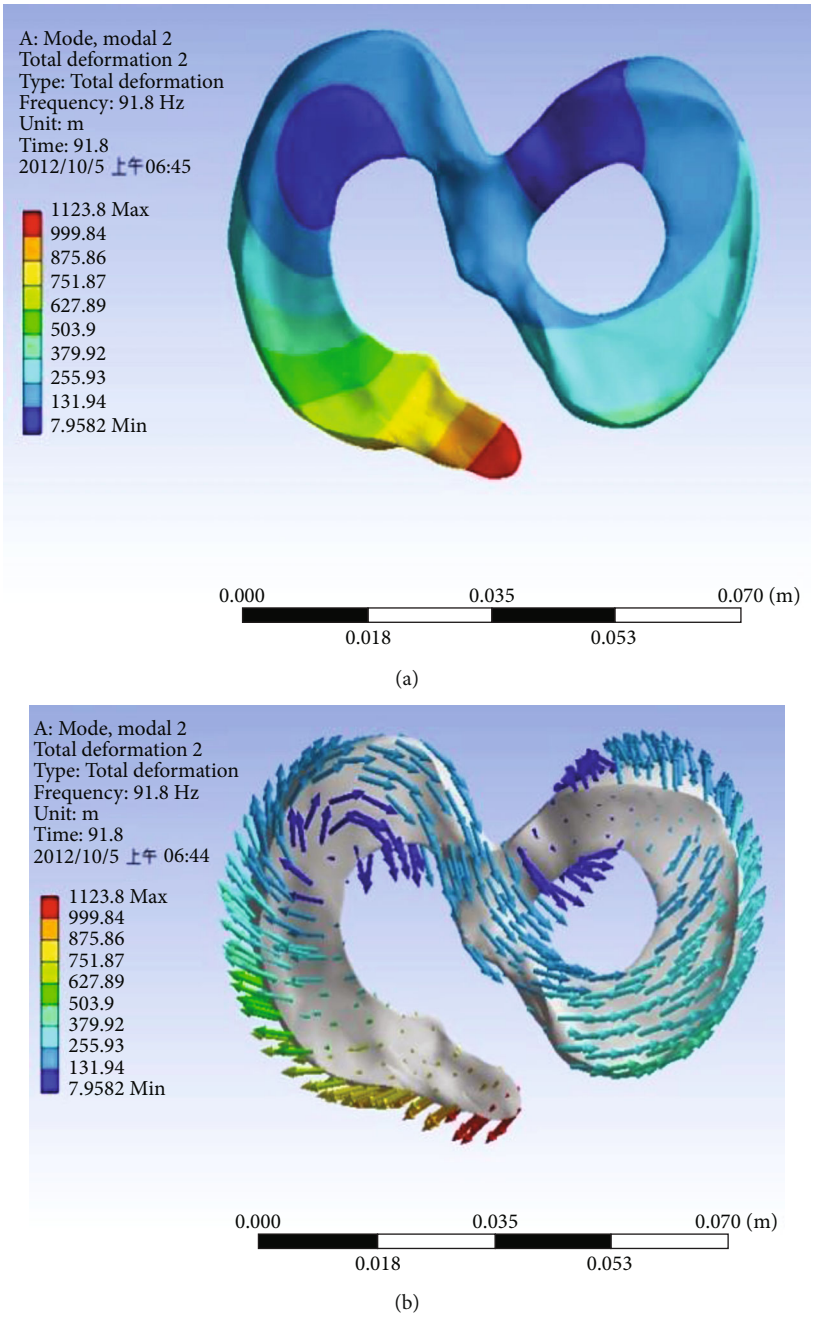

Figure 6: Second mode shape of meniscus model at 91.8 Hz (shrinkage–expansion vibration in the surface perpendicular to thickness direction). (a) Second mode shape. (b) Vector plot of second mode shape.

the FEM calculated natural frequency with the experimental result provided by Wakeling, and (3) to analyze the fatigue of the meniscus within the CKM which can better simulate the real situation of leg movement.

2.3. Material Properties. Real human bone and different soft tissue (meniscus, fibrochondrocytes, etc.) material parameters [29–34] (Table 1), such as Young's modulus, Poisson's ratio, and density, are set in the FEM models. Soft tissues usually exhibit significant damping. The damping ratio is set 0.1 in this case. The meniscus is modelled as isotropic single-phase linear elastic material with an elastic (Young's) modulus (E) of 59 MPa and a Poisson's ratio (ν) of 0.45. The articular cartilage is the smooth, white tissue that covers the ends of bones, for instance, the femur and tibia, where they come together to form joints. To simplify the problem in this study, they are neglected in the model and are segmented as unique parts with their relative femur and tibia structures. Hence, they are not segmented as separated parts.

2.4. Boundary Conditions. The boundary conditions are set "free" around the boundary of the meniscus model in FEM modal analysis for obtaining natural frequencies and mode shapes. The free boundary condition means no loads or

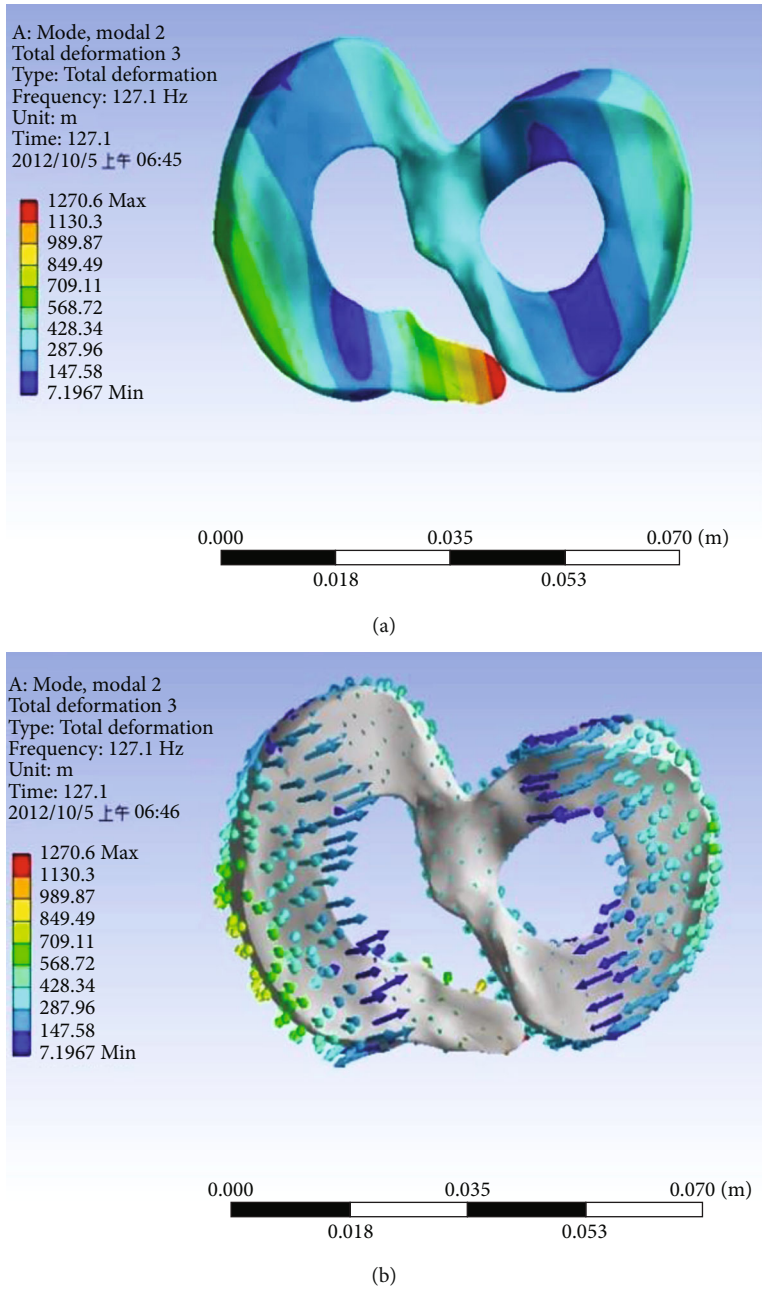

Figure 7: Third mode shape of meniscus model at 127.1 Hz (bending vibration via thickness direction). (a) Third mode shape. (b) Vector plot of third mode shape.

constraints applied on the surface of the 3D meniscus model. Hence, along with many flexible body modes, there are six rigid body modes found by FEM: three translation modes and three rotation modes along with x, y, and z-axis, respectively. These rigid body modes do not have a relative displacement between each molecule of the meniscus. So they possess zero natural frequency theoretically.

To simulate the real situation of leg movement, the fatigue life analysis of meniscus is carried out by combining the current meniscus model and other parts of the knee model, which was built by the authors' previous work, to form a CKM. The boundary conditions of this CKM are assigned fixed at the femur head-hip position and free otherwise. For fatigue analysis, the cyclic loads of 1,000 N were applied on the distal tibia to represent the repeated ground reaction force to the leg during movement.

2.5. Convergence Criterion. In finite element analysis, solution accuracy is judged in terms of convergence as the element "mesh" is refined. Mesh refinement is one of the essential issues in computational mechanics to assure accuracy. It is related to how small the elements need to be, while the results are not affected by changing the size of the mesh. Usually, the procedure repeats the analysis with progressively reduced mesh size until the variation of the analyzed parameter value, natural frequency for this case, becomes less than a

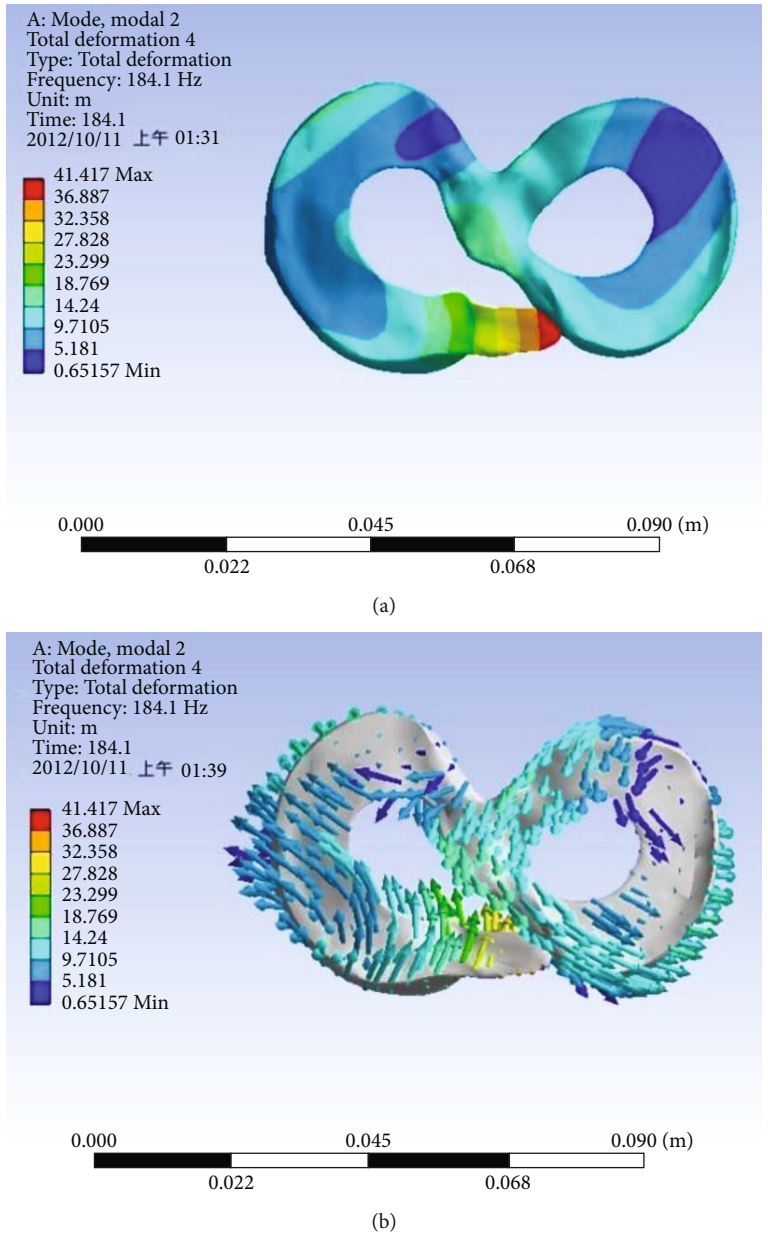

Figure 8: Fourth mode shape of meniscus model at 184.1 Hz (bending vibration via thickness direction). (a) Fourth mode shape. (b) Vector plot of fourth mode shape.

certain percentage, under 5% for instance [35–37]. Then, the mesh size is evaluated to be optimal, and the analysis result is determined to be accurate. This research performs the mesh elements convergence test to find the optimal element size before the analysis. If the convergence analysis diagram presents a divergence phenomenon, one must return to the preprocess section; adjust the settings of material parameters, contact conditions, or boundary conditions; and begin to re-analyze again. Fundamental natural frequency is used to exam the convergence of the model. The convergence criterion is specified to be less than 5% of the variation of the frequencies when increasing the mesh elements. This article investigates the convergence test of the mesh elements for the first natural frequency of meniscus referring to the authors' previous work [25]. When the number of elements is greater than 3,500, the first natural frequency of meniscus converges to 72.4 Hz. Therefore, this study adopts 3,500 FE elements for the modal analysis of the meniscus.

On the other hand, the first natural frequency of CKM converged to 17.25 Hz at 40,000 elements. It is convinced to use those elements for fatigue life analysis. Also, since the CKM is not a sturdy structure, with mere ligaments and meniscal soft tissues supporting the knee, its first natural frequency is relatively low (17.25 Hz).

3. Results and Discussion

3.1. Comparison of the First Natural Frequency of the CKM Model with Other Papers. Wakeling et al. [38] used a hydraulic shaker to stimulate the human leg at the foot end and

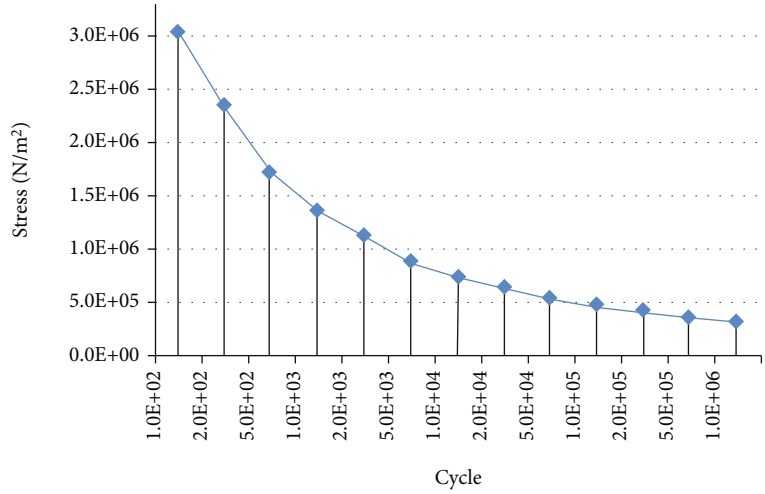

Figure 9: Meniscus S-N curve used for meniscus fatigue analysis.

conducted the modal test of the lower extremity via accelerometers. The average measured experimental data of the first natural frequency of the lower extremity is 15.25 Hz. This data is very close to our FEM calculated first natural frequency, 17.25 Hz, of the CKM model (refer to the convergence criterion section). The difference between the two data is around 11.6%. This promising result proves that both the CKM and meniscus models are acceptable for the dynamic analysis.

3.2. Modal Analysis Results of Meniscus Model. The modal analysis of the meniscus alone model is achieved under a free boundary condition. There is an infinite number of natural frequencies in a continuous structure. Only the first few lower modes are significant and will be discussed in the analysis. The first six zero-frequency modes are rigid body modes and will not be discussed here. Table 2 shows the first four flexible vibration natural frequencies of the meniscal model.

Because it is a thin and small structure, the natural frequencies of the meniscus are as high as 72.4 Hz and above. Figure 5(a) shows the first mode shape of the meniscus model at 72.4 Hz, bending vibration mode through-thickness direction. The maximum displacement occurs at the front-end tip of the meniscus. Figure 6(a) shows the second mode shape of the meniscus model at 91.8 Hz, in-plane shrinkage–expansion vibration mode in the surface perpendicular to the thickness direction. The maximum displacement occurs at the front-end tip of the meniscus. Figure 7(a) shows the third mode shape of the meniscus model at 127.1 Hz, bending vibration mode through-thickness direction. Two parallel nodal lines are tilt in the southeastern direction. The maximum displacement occurs at two sides and the front-end tip of the meniscus. Figure 8(a) shows the fourth mode shape of the meniscus model at 184.1 Hz, bending vibration mode through-thickness direction. Two parallel nodal lines are tilt in the northeastern direction. The maximum displacement occurs at the lower-left open end of the meniscus. One should remember that each natural (resonance) frequency has a corresponding mode. The displacement scale of each vibration mode is magnified thousands of times to distinguish the nodal area and vibration part, as shown in Figures 6–9.

On the right-hand side of Figures 5(b)–8(b), the deformation vector plots of the first to fourth mode are shown, respectively. The vector plot is another way to view the deformation of the vibrating body.

The system design engineers are trained to examine the natural frequencies and mode shapes of the structure. They will like to or even change the design to avoid the natural frequencies, resonance, when the structure is in the motion circumstance. When the structure is in a resonance situation, the vibration displacement will grow with time until fracture happened.

A lot of papers discussing cell-based tissue engineering from a micro point of view instead of a macro point of view as this study. Therefore, hardly could we find similar studies about modal and fatigue analysis with similar conditions in the literature to compare with. It is suggested that the synthesis human meniscus model manufactured by 3B Incorporation, made in plastic material (polypropylene), can be used to execute the experimental modal analysis. The measured fundamental natural frequency can be compared with the one by finite element analysis in this study. The estimated difference between them should be under 15%, according to Wakeling's result mentioned above.

3.3. Fatigue Analysis Results of Meniscus Model. It is hard to find the fatigue analysis of human meniscus in reference. The material properties include the ultimate strength of 6.23 MPa, the tensile strength of 5.8 MPa [39], and the compressive strength of 3.27 MPa [12] of knee joint cartilage, which is employed to simulate the real motion of the human meniscus in the knee joint [40, 41]. The maximum stress of 3.0 MPa, corresponding to a cyclic load of 1000 N, is used to obtain the meniscus fatigue S-N (stress vs. number of cycles) curve, as shown in Figure 9. The finite element ANSYS fatigue solver utilizes this meniscus S-N curve to calculate the meniscus fatigue analysis.

Figure 10(a) shows the stress distribution diagram of meniscus life analysis. The blue color regions represent long

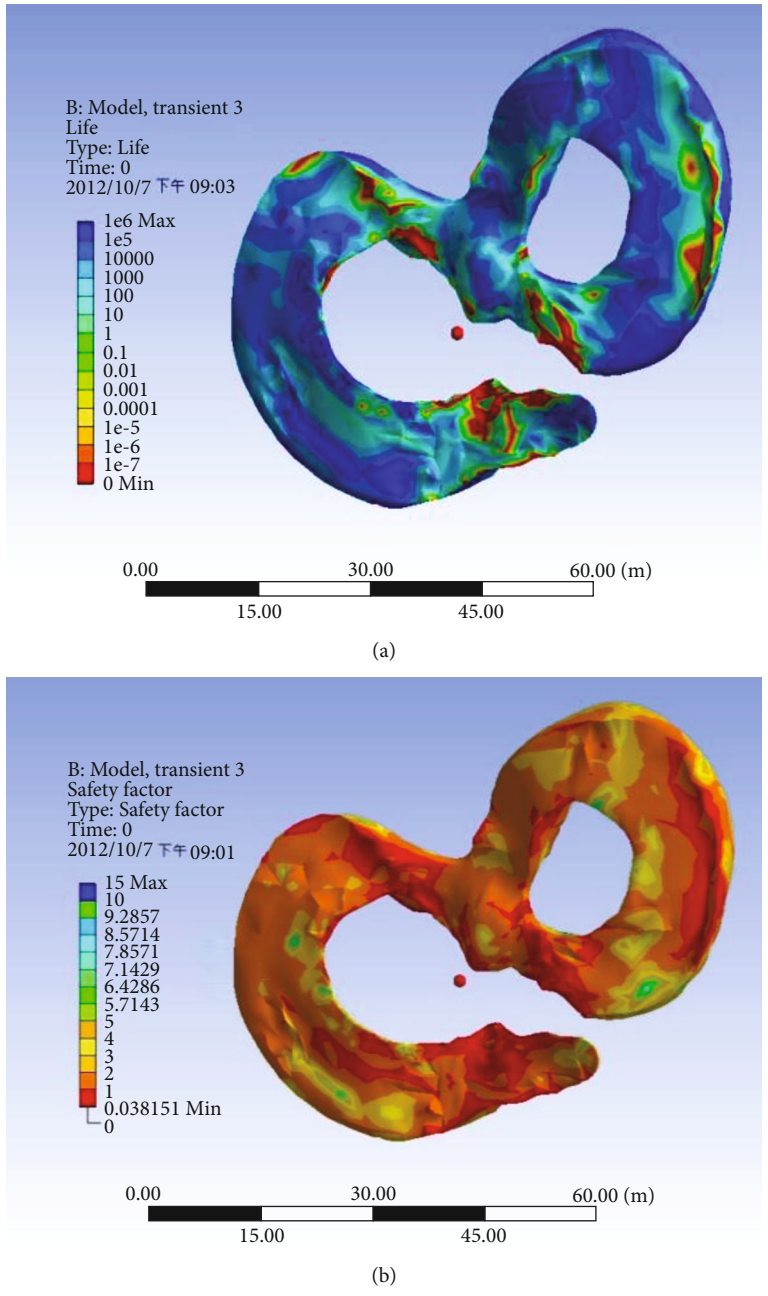

Figure 10: Stress distribution of meniscus under fatigue life analysis. (a) Available cycle. (b) Safety factor.

life, i.e. sustain tens of millions of cycles loading of the meniscus. A few red color spots are stress concentration due to scanned model roughness and should be eliminated from the FEM. Figure 10(b) presents the safety factor fatigue simulation. The most orange color region indicates that life analysis can reach the safety factor of 1.5 as acceptable by normal practice. The abovementioned stress concentration issue also causes fewer red spots of lower safety factors.

3.4. Limitations. This is the first study using natural frequency, mode shape, and fatigue analysis for the human meniscus in the literature. The results of this study can be applied to do subsequent knee dynamic simulation analysis, to reduce the knee joint and lower external impacts, and to manufacture artificial meniscus through tissue engineering. Nevertheless, these results should be interpreted with caution because of several limitations in this study. First, we only considered one size of the "meniscus sample" here. Second, the scanned surface are the ones of a model of the menisci and not of the menisci themselves. Third, the authors characterize the mechanical characteristics of the meniscus as the isotropic single-phase linear elastic material. It is prospected to consider the viscoelasticity of the tissue in the future work [42–44]. Hence, future studies with an improved design and

better control of confounding factors are required to enable a more thorough understanding.

4. Conclusions

The normal mode and fatigue life analysis of the meniscus is obtained by FEM ANSYS simulation. After confirming the correctness of the FEM model, real human hard and soft tissue material parameters are substituted into the model to analyze the normal mode and fatigue life of the real knee joint. Several interesting points are summarized as follows:

(1) This article finds the fundamental natural frequencies of the meniscus, although it is a thin flat structure. In-plane and out-of-plane normal modes of the meniscus model are found. Relative maximum displacement often occurred at the open-end tip of the left hole in the modal analysis. The designer should identify the fundamental normal modes of the artificial meniscus to avoid resonance effects.

(2) Available cycle and safety factor of life analysis, obtained from meniscus, are shown as stress distribution diagrams, respectively.

(3) The achieved results can be applied to do subsequent knee dynamic simulation analysis, to reduce the knee joint and lower external impacts, and to manufacture artificial meniscus through tissue engineering.

Data Availability

The simulation data of the above article used to support the findings of this study have not been made available because of two reasons described as follows: (1) the results were obtained using the authorized software. (2) Any data usage should comply with the Intellectual Property Rights related regulations of the Ministry of Science and Technology of Taiwan, which is the financially supported organization of this study.

Conflicts of Interest

The authors declare that there is no conflict of interest regarding the publication of this paper.

Acknowledgments

This research was financially supported by the Ministry of Science and Technology, Taiwan, R.O.C. [MOST 109-2221-E-230-002].

References

[1] National Center for Chronic Disease Prevention and Health Promotion (NCCDPHP) and Centers for Disease Control and Prevention (CDC), USA, "Arthritis: How CDC Improves Quality of Life for People With Arthritis," https://www.cdc.gov/chronicdisease/resources/publications/factsheets/arthritis.htm.

[2] A. I. Bochynska, T. G. Van Tienen, G. Hannink, P. Buma, and D. W. Grijpma, "Development of biodegradable hyperbranched tissue adhesives for the repair of meniscus tears," *Acta Biomaterialia*, vol. 32, pp. 1–9, 2016.

[3] B. Bilgen, C. T. Jayasuriya, and B. D. Owens, "Current concepts in meniscus tissue engineering and repair," *Advanced Healthcare Materials*, vol. 7, no. 11, article e1701407, 2018.

[4] P. Buma, N. N. Ramrattan, T. G. van Tienen, and R. P. H. Veth, "Tissue engineering of the meniscus," *Biomaterials*, vol. 25, no. 9, pp. 1523–1532, 2004.

[5] H. Pereira, S. G. Caridade, A. M. Frias et al., "Biomechanical and cellular segmental characterization of human meniscus: building the basis for tissue engineering therapies," *Osteoarthritis and Cartilage*, vol. 22, no. 9, pp. 1271–1281, 2014.

[6] B. Zielinska and T. L. Donahue, "3D finite element model of meniscectomy: changes in joint contact behavior," *Journal of Biomechanical Engineering*, vol. 128, no. 1, pp. 115–123, 2006.

[7] T.-M. Guess, G. Thiagarajan, M. Kia, and M. Mishra, "A subject specific multibody model of the knee with menisci," *Medical Engineering & Physics*, vol. 32, no. 5, pp. 505–515, 2010.

[8] C.-H. Kuo, *Effect of ACL Strength on Stress Distribution of Meniscus when Landing from a Jump, [M.S. thesis]*, Institute of Biomedical Engineering, National Yang Ming University, Taipei, Taiwan, 2008.

[9] L. P. Räsänen, P. Tanska, M. E. Mononen et al., "Spatial variation of fixed charge density in knee joint cartilage from sodium MRI–implication on knee joint mechanics under static loading," *Journal of Biomechanics*, vol. 49, no. 14, pp. 3387–3396, 2016.

[10] J. R. Meakin, N. G. Shrive, C. B. Frank, and D. A. Hart, "Finite element analysis of the meniscus: the influence of geometry and material properties on its behaviour," *The Knee*, vol. 10, no. 1, pp. 33–41, 2003.

[11] M. Freutel, H. Schmidt, L. Dürselen, A. Ignatius, and A. F. Galbusera, "Finite element modeling of soft tissues: material models, tissue interaction and challenges," *Clinical Biomechanics*, vol. 29, no. 4, pp. 363–372, 2014.

[12] M. Z. Bendjaballah, A. Shirazi-AdI, and D. J. Zukor, "Biomechanics of the human knee joint in compression: reconstruction, mesh generation and finite element analysis," *The Knee*, vol. 2, no. 2, pp. 69–79, 1995.

[13] W. T. Thomson and M. D. Dahleh, *Theory of Vibration with Applications Fourth Edition, eBook*, CRC Press, London, 2018.

[14] H. Pereira, A. M. Frias, S. G. Caridade et al., "443 cellular and biomechanical segmental characterization of human meniscus," *Osteoarthritis and Cartilage*, vol. 19, no. S1, p. S205, 2011.

[15] W. Niu, W. Guo, S. Han, Y. Zhu, S. Liu, and Q. Guo, "Cell-Based Strategies for Meniscus Tissue Engineering," *Stem Cells International*, vol. 2016, Article ID 4717184, 10 pages, 2016.

[16] M. Cucchiarini, A. L. McNulty, R. L. Mauck, L. A. Setton, F. Guilak, and H. Madry, "Advances in combining gene therapy with cell and tissue engineering-based approaches to enhance healing of the meniscus," *Osteoarthritis and Cartilage*, vol. 24, no. 8, pp. 1330–1339, 2016.

[17] C. Scotti, M. T. Hirschmann, P. Antinolfi, I. Martin, and G. M. Peretti, "Meniscus repair and regeneration: review on current methods and research potential," *European Cells & Materials*, vol. 26, pp. 150–170, 2013.

[18] A. Szojka, K. Lalh, S. H. J. Andrews, N. M. Jomha, M. Osswald, and A. B. Adesida, "Biomimetic 3D printed scaffolds for meniscus tissue engineering," *Bioprinting*, vol. 8, pp. 1–7, 2017.

[19] T. D. Stocco, E. Antonioli, M. L. Romagnolli, G. F. Sousa, M. Ferretti, and A. O. Lobo, "Aligned biomimetic scaffolds based on carbon nanotubes-reinforced polymeric nanofibers for knee meniscus tissue engineering," *Materials Letters*, vol. 264, article 127351, 2020.

[20] S.-W. Kang, S.-M. Son, J.-S. Lee et al., "Regeneration of whole meniscus using meniscal cells and polymer scaffolds in a rabbit total meniscectomy model," *Journal of Biomedical Materials Research—Part A*, vol. 78, no. 3, pp. 659–671, 2006.

[21] B. B. Mandal, S.-H. Park, E. S. Gil, and D. L. Kaplan, "Multilayered silk scaffolds for meniscus tissue engineering," *Biomaterials*, vol. 32, no. 2, pp. 639–651, 2011.

[22] M. B. Pabbruwe, W. Kafienah, J. F. Tarlton, S. Mistry, D. J. Fox, and A. P. Hollander, "Repair of meniscal cartilage white zone tears using a stem cell/collagen-scaffold implant," *Biomaterials*, vol. 31, no. 9, pp. 2583–2591, 2010.

[23] T. Villa, F. Migliavacca, D. Gastaldi, M. Colombo, and R. Pietrabissa, "Contact stresses and fatigue life in a knee prosthesis: comparison between in vitro measurements and computational simulations," *Journal of Biomechanics*, vol. 37, no. 1, pp. 45–53, 2004.

[24] B. V. Murlimanju, N. Narga, K. Ashwin et al., "The anterior transverse ligament of knee: morphological and morphometric study in formalin fixed human fetuses," *Journal of Surgical Academy*, vol. 4, no. 2, pp. 24–28, 2014.

[25] P.-P. Yu, J.-G. Tseng, M.-Y. Huang, and B.-W. Huang, "Injury assessment via stress analysis of the human knee joint," *Journal of Vibroengineering*, vol. 19, no. 5, pp. 3832–3841, 2017.

[26] J.-G. Tseng, B. Huang, S.-H. Liang, K. Yen, and Y. C. Tsai, "Normal mode analysis of human fibula," *Life Science Journal*, vol. 11, no. 12, pp. 711–718, 2014.

[27] A. N. Damira, A. Elkhatibb, and G. Nassef, "Prediction of fatigue life using modal analysis for grey and ductile cast iron," *International Journal of Fatigue*, vol. 29, no. 3, pp. 499–507, 2007.

[28] I. Fernandez, J. M. Bairán, and A. R. Mari, "3D FEM model development from 3D optical measurement technique applied to corroded steel bars," *Construction and Building Materials*, vol. 124, pp. 519–532, 2016.

[29] R. A. Stockwell, "The cell density of human articular and costal cartilage," *Journal of Anatomy*, vol. 101, no. 4, pp. 753–763, 1967.

[30] M. B. Goldring, "Chapter 3 - cartilage and chondrocytes," in *Kelley's Textbook of Rheumatology, Vol. I*, pp. 33.e10–60.e10, Elsevier Inc., 2013.

[31] P. Bursac, A. M. York, J. M. Deuerling, P. M. Kuznia, and J. R. Bianchi, "Dynamic and static mechanical properties of human meniscus in tension and compression: relationships with tissue composition," *52nd Annual Meeting of the Orthopaedic Research Society*, 2005, Paper No: 0030, Corpus ID: 38446897.

[32] Y. Liang, E. Idrees, S. H. J. Andrews et al., "Plasticity of human meniscus fibrochondrocytes: a study on effects of mitotic divisions and oxygen tension," *Scientific Reports*, vol. 7, no. 1, article 12148, 2017.

[33] Y.-G. Chang, *3D FEM Analysis of the Total Knee Prosthesis with Reserved Anterior and Posterior Cruciate Ligament*, PLA Postgraduate Medical School, General Hospital of the Chinese People's Liberation Army, 2008.

[34] S.-H. Liang, *Dynamic Characteristics of the Human Leg, [M.S. thesis]*, Graduate Institute of Mechatronics Engineering, Cheng Shiu University, Kaohsiung, Taiwan, 2011.

[35] D. Jung, D. Lee, M. Kim, H. Kim, and S. K. Park, "Mesh convergence test system in integrated platform environment for finite element analysis," *The Journal of Supercomputing*, vol. 76, no. 7, pp. 5244–5258.

[36] T. J. R. Hughes, *The finite element method: linear static and dynamic finite element analysis, Chap. 5, 8, 10*, Dover Publications, Mineola, NY, 2000.

[37] K.-J. Bathe, *Finite Element Procedures, Chap 4-7, 2nd Edition: Fourth Printing*, Prentice Hall, Pearson Education, Inc, New York, NY, USA, 2016.

[38] J. M. Wakeling, B. M. Nigg, and A. I. Rozitis, "Muscle activity damps the soft tissue resonance that occurs in response to pulsed and continuous vibrations," *Journal of Applied Physiology*, vol. 93, no. 3, pp. 1093–1103, 2002.

[39] M. Tissakht and A. M. Ahmed, "Tensile stress-strain characteristics of the human meniscal material," *Journal of Biomechanics*, vol. 28, no. 4, pp. 411–422, 1995.

[40] G. Tao, Y. Tian-fu, and X. Jie, "Biomechanics study of polyvinyl alcohol hydrogel/nano-hydroxyapatite + polyamide 66 in repair of articular cartilage and subchondral bone defects," *Journal of Clinical Rehabilitative Tissue Engineering Research*, vol. 12, no. 6, pp. 1051–1054, 2008.

[41] Y. Liu, "Experiment study for resurfacing cartilage defect with new biphasic biomaterials, [Ph.D. Dissertation]," Si-Chuan University, China, 2007.

[42] L. Camarda, E. Bologna, D. Pavan et al., "Posterior meniscal root repair: a biomechanical comparison between human and porcine menisci," *Muscles, Ligaments & Tendons Journal*, vol. 9, no. 1, 2019.

[43] E. Bologna, M. Di Paola, K. Dayal, L. Deseri, and M. Zingales, "Fractional-order nonlinear hereditariness of tendons and ligaments of the human knee," *Philosophical Transactions of the Royal Society A*, vol. 378, no. 2172, article 20190294, 2020.

[44] M. Shemesh and R. Asher, "Viscoelastic properties of a synthetic meniscus implant, *viscoelastic properties of a synthetic meniscus implant*," *Journal of the Mechanical Behavior of Biomedical Materials*, vol. 29, pp. 42–55, 2014.